Inorg. Chem. **2006**, *45*, 1617–1626

Anion Influence on the Structures of a Series of Copper(II) Metal–Organic Frameworks

Pilar Díaz,[†] Jordi Benet-Buchholz,[‡] Ramón Vilar,*[,‡,§] and Andrew J. P. White[†]

Department of Chemistry, Imperial College London, South Kensington, London SW7 2AZ, United Kingdom, Institute of Chemical Research of Catalonia (ICIQ), 43007 Tarragona, Spain, and Institution of Research and Advanced Studies of Catalonia (ICREA), 08010 Barcelona, Spain

Received August 26, 2005

The main aim of the work herein presented is to investigate the influence of different anions on the overall structure of a series of metal–organic frameworks. The reactions between $CuCl_2$, $Cu(OAc)_2$, and $CuSO_4$ and the two bipyridylurea ligands **L¹** and **L²** [**L¹** = 1,3-bis(pyridin-4-ylmethyl)urea; **L²** = 1,3-bis(pyridin-3-ylmethyl)urea; see Scheme 1 in paper] have been carried out and the crystal structure of five of the resulting metal–organic assemblies determined. These crystal structures have shown that the geometry and size of the corresponding anions together with their coordinating and hydrogen-bonding properties are essential in determining the final structures of the assemblies. Particularly interesting, because of their potential as nanoporous materials, are the assemblies obtained from the reaction between each of the two ligands (**L¹** and **L²**) and $CuCl_2$, which yield noninterpenetrating 2D metal–organic layers made of squares of ca. 15 × 15 Å. These layers stack on top of each other, producing infinite 3D channels filled with solvent molecules. The thermal stabilities of the five metal–organic frameworks prepared have been studied by means of thermogravimetric analysis. Preliminary X-ray powder diffraction studies of one of these metal–organic frameworks indicate that upon heating the assembly changes to a different crystalline structure. Interestingly, the original structure reforms upon exposure of this sample to traces of water.

Introduction

The synthesis of metal−organic coordination networks is a very active area of current research.[1−6] This is due to the fundamental interest there is in understanding self-assembly processes and also due to the potential applications that the resulting metal−organic hybrid materials can have. Because many of these networks have large cavities and surface areas, there is interest in using them for storage,[7−12] sensing,[13,14] and catalysis.[15−18] Furthermore, metal centers can confer interesting optical and magnetic properties to the assemblies, which can lead to the preparation of novel functional materials.

In order for these applications to be realized, it is essential to have efficient synthetic methodologies to prepare these frameworks. Because of the dynamic nature of the metal−ligand bonds and the various potential geometries around

* To whom correspondence should be addressed at ICIQ. E-mail: rvilar@iciq.es. Tel: +34 977 920 212. Fax: +34 977 920 228.
† Imperial College London.
‡ ICIQ.
§ ICREA.

(1) Rosseinsky, M. J. *Microporous Mesoporous Mater.* **2004**, *73*, 15.
(2) Eddaoudi, M.; Moler, D. B.; Li, H.; Chen, B.; Reineke, T. M.; O'Keeffe, M.; Yaghi, O. M. *Acc. Chem. Res.* **2001**, *34*, 319.
(3) James, S. L. *Chem. Soc. Rev.* **2003**, *32*, 276.
(4) Moulton, B.; Zaworotko, M. J. *Chem. Rev.* **2001**, *101*, 1629.
(5) Papaefstathiou, G. S.; MacGillivray, L. R. *Coord. Chem. Rev.* **2003**, *246*, 169.
(6) Rowsell, J. L. C.; Yaghi, O. M. *Microporous Mesoporous Mater.* **2004**, *73*, 3.
(7) Bu, X.-H.; Tong, M.-L.; Chang, H.-C.; Kitagawa, S.; Batten, S. R. *Angew. Chem., Int. Ed.* **2003**, *43*, 192.
(8) Janiak, C. *Angew. Chem., Int. Ed. Engl.* **1997**, *36*, 1431.
(9) Noro, S.-i.; Kitagawa, S.; Kondo, M.; Seki, K. *Angew. Chem., Int. Ed.* **2000**, *39*, 2082.
(10) Chen, B.; Ockwig, N. W.; Millward, A. R.; Contreras, D. S.; Yaghi, O. M. *Angew. Chem., Int. Ed.* **2005**, *44*, 4745.
(11) Rowsell, J. L. C.; Yaghi, O. M. *Angew. Chem., Int. Ed.* **2005**, *44*, 4670.
(12) Sudik, A. C.; Millward, A. R.; Ockwig, N. W.; Cote, A. P.; Kim, J.; Yaghi, O. M. *J. Am. Chem. Soc.* **2005**, *127*, 7110.
(13) Maspoch, D.; Ruiz-Molina, D.; Wurst, K.; Domingo, N.; Cavallini, M.; Biscarini, F.; Tejada, J.; Rovira, C.; Veciana, J. *Nat. Mater.* **2003**, *2*, 190.
(14) Halder, G. J.; Kepert, C. J.; Moubaraki, B.; Murray, K. S.; Cashion, J. D. *Science* **2002**, *298*, 1762.
(15) Janiak, C. *Dalton Trans.* **2003**, 2781.
(16) Lin, W. *J. Solid State Chem.* **2005**, *178*, 2486.
(17) Wu, C.-D.; Hu, A.; Zhang, L.; Lin, W. *J. Am. Chem. Soc.* **2005**, *127*, 8940.
(18) Schlichte, K.; Kratzke, T.; Kaskel, S. *Microporous Mesoporous Mater.* **2004**, *73*, 81.

10.1021/ic051457i CCC: $33.50
Published on Web 01/18/2006

the metal centers, it is often difficult to predict the exact nature of the final metal−organic assemblies. Their structures are highly dependent on the geometry, bulkiness, and flexibility of the ligands that are used as building blocks. Furthermore, the experimental conditions employed (such as the solvent, temperature, and crystallization method) and the nature of the metal's counterions can also have an important impact on the structure of the final assembly. Anions can influence the structure either by coordinating directly to the metal centers or by acting as templates that preorganize the organic building blocks used to build up the assembly. For example, Hannon et al. have published a systematic study of the role played by different anions on the self-assembly of Ag^I and a terpyridine-based ligand.[19] When different silver salts are reacted with the ligand under the same experimental conditions, a range of monomeric and polymeric species were obtained. Min and Suh have reported another interesting example of anion-directed assembly of Ag^I extended structures by using the multipodal ligand ethylenediamine−tetrapropionitrile.[20] The reaction between this ligand and $AgNO_3$, $Ag(CF_3SO_3)$, or $AgClO_4$ yielded a 1D chain, a 2D layer, or a 2D network, respectively. An interesting aspect of these systems is that they display anion-induced interconversion in the crystalline state. Other relevant examples showing the influence of the anionic counterions on the final structure of the assembly have been reported by Champness and Schröder,[21,22] Keller,[23,24] Champness,[25,26] and Ciani,[27] among others.[28−31]

As part of our ongoing interest in understanding the ability of anions to direct the assembly of metal−organic systems,[32−35] we have recently engaged in studying the influence that a range of anionic species have on the structure of a series of metal coordination networks with bipyridyl ligands that contain hydrogen-bonding groups. It has been previously established that both $\mathbf{L^1}$ and $\mathbf{L^2}$ [$\mathbf{L^1}$ = 1,3-bis(pyridin-4-ylmethyl)urea; $\mathbf{L^2}$ = 1,3-bis(pyridin-3-ylmethyl)urea; see Schemes 1 and 2] react with $AgBF_4$, $AgNO_3$, $Cd(NO_3)_2$, and $Cu(NO_3)_2$ to yield coordination polymers.[36,37] However, no systematic study has been carried out to determine the role that the counteranions play in determining the structure of the final assemblies. Herein, the synthesis and X-ray crystal structure of five new coordination networks formed upon mixing different copper(II) salts with the ligands $\mathbf{L^1}$ and $\mathbf{L^2}$ (see Schemes 1 and 2) are presented. The influence of the anionic counterions on the final structure of the assemblies is discussed. The thermal stabilities of the new metal−organic networks, studied using thermogravimetric analysis (TGA), are also reported.

Scheme 1. Summary of the Products Obtained from the Reactions between Different Copper(II) Salts and the Bipyridyl Ligand $\mathbf{L^1}$

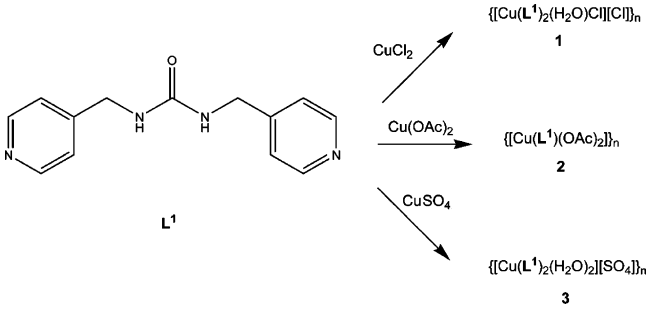

Scheme 2. Summary of the Products Obtained from the Reactions between Different Copper(II) Salts and the Bipyridyl Ligand $\mathbf{L^2}$

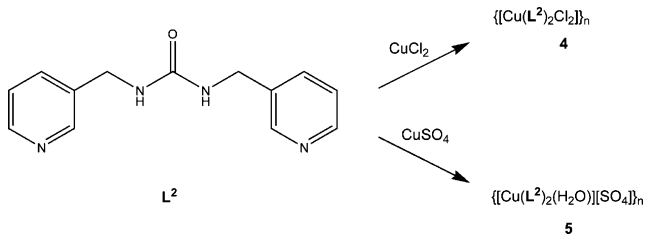

Results and Discussion

Synthesis and Single-Crystal X-ray Structures of 1−3. The reaction between $\mathbf{L^1}$ and $Cu(NO_3)_2$ has been previously[37] shown to yield a coordination network with formula $[Cu(\mathbf{L^1})_2(H_2O)(NO_3)][NO_3]$. In this assembly, one of the nitrate anions is directly coordinated to the metal center, while the other one is outside the coordination sphere, interacting via hydrogen bonds with the urea groups of the ligand. This suggests that the overall structure of the coordination network is very much influenced by the nature of the anion (geometry and coordinating ability). Consequently, to study systematically the role of the counteranions in the formation of the metalla-assemblies, the reactions between three different copper(II) salts (see Scheme 1) and $\mathbf{L^1}$ were studied. The infinite metal−organic assemblies **1**−**3** were generated by

(19) Hannon, M. J.; Painting, C. L.; Plummer, E. A.; Childs, L. J.; Alcock, N. W. *Chem.—Eur. J.* **2002**, *8*, 2225.
(20) Min, K. S.; Suh, M. P. *J. Am. Chem. Soc.* **2000**, *122*, 6834.
(21) Blake, A. J.; Baum, G.; Champness, N. R.; Chung, S. S. M.; Cooke, P. A.; Fenske, D.; Khlobystov, A. N.; Lemenovskii, D. A.; Li, W.-S.; Schröder, M. *Dalton Trans.* **2000**, 4285.
(22) Khlobystov, A. N.; Blake, A. J.; Champness, N. R.; Lemenovskii, D. A.; Majouga, A. G.; Zyk, N. V.; Schröder, M. *Coord. Chem. Rev.* **2001**, *222*, 155.
(23) Inman, C.; Knaust, J. M.; Keller, S. W. *Chem. Commun.* **2002**, 156.
(24) Lopez, S.; Keller, S. W. *Inorg. Chem.* **1999**, *38*, 1883.
(25) Oxtoby, N. S.; Blake, A. J.; Champness, N. R.; Wilson, C. *Proc. Natl. Acad. Sci. U.S.A.* **2002**, *99*, 4905.
(26) Blake, A. J.; Champness, N. R.; Cooke, P. A.; Nicolson, J. E. B.; Wilson, C. *Dalton Trans.* **2000**, 3811.
(27) Carlucci, L.; Ciani, G.; Proserpio, D. M.; Sironi, A. *Inorg. Chem.* **1998**, *37*, 5941.
(28) He, C.; Zhang, B.-G.; Duan, C.-Y.; Li, J.-H.; Meng, Q.-J. *Eur. J. Inorg. Chem.* **2000**, 2549.
(29) Jung, O.-S.; Kim, Y. J.; Lee, Y.-A.; Park, J. K.; Chae, H. K. *J. Am. Chem. Soc.* **2000**, *122*, 9921.
(30) Kang, Y.; Lee, S. S.; Park, K.-M.; Lee, S. H.; Kang, S. O.; Ko, J. *Inorg. Chem.* **2001**, *40*, 7027.
(31) Schauer, C. L.; Matwey, E.; Fowler, F. W.; Lauher, J. W. *J. Am. Chem. Soc.* **1997**, *119*, 10245.
(32) Vilar, R.; Mingos, D. M. P.; White, A. J. P.; Williams, D. J. *Chem. Commun.* **1999**, 229.
(33) Vilar, R.; Mingos, D. M. P.; White, A. J. P.; Williams, D. J. *Angew. Chem., Int. Ed.* **1998**, *37*, 1258.
(34) Cheng, S.-T.; Doxiadi, E.; Vilar, R.; White, A. J. P.; Williams, D. J. *J. Chem. Soc., Dalton Trans.* **2001**, 2239.
(35) Diaz, P.; Mingos, D. M. P.; Vilar, R.; White, A. J. P.; Williams, D. J. *Inorg. Chem.* **2004**, *43*, 7597.
(36) Schauer, C. L.; Matwey, E.; Fowler, F. W.; Lauher, J. W. *Cryst. Eng.* **1999**, *1*, 213.
(37) Plater, M. J.; de Silva, B. M.; Skakle, J. M. S.; Howie, R. A.; Riffat, A.; Gelbrich, T.; Hursthouse, M. B. *Inorg. Chim. Acta* **2001**, *325*, 141.

Table 1. Crystallographic Data and Details of the Structure Solution and Refinement Procedures for **1**−**5**

compd	**1**	**2**	**3**	**4**	**5**
formula	$C_{26}H_{30}N_8O_3Cu_1Cl_1\cdot xH_2O$	$C_{17}H_{20}CuN_4O_5$	$[C_{26}H_{32}CuN_8O_4](SO_4)\cdot 2H_2O$	$C_{26}H_{28}Cl_2CuN_8O_2\cdot 7H_2O$	$C_{26}H_{30}N_8O_3Cu_1\cdot xH_2O$
fw [g mol^{-1}]	794.56	423.91	716.23	745.12	758.56
T [K]	90	293	173	173	100
λ, Å	1.541 78	1.542 48	1.542 48	1.542 48	0.710 73
space group	$P2_1/n$	$P2_1/n$	$C2/c$	$P2_1/c$	$Pba2$
a [Å]	9.1072(2)	9.2047(5)	13.6925(7)	11.0549(6)	18.4192(10)
b [Å]	23.9835(7)	18.3674(10)	47.613(2)	21.4021(9)	20.4123(11)
c [Å]	18.0800(5)	10.8366(7)	14.3110(9)	15.4420(10)	8.9376(5)
β [deg]	97.563(2)	93.798(5)	105.693(5)	105.118(5)	
V [Å^3]	3914.72(18)	1828.08(18)	8982.2(8)	3527.1(3)	3360.3(3)
Z	4	4	12	4	4
d_{calcd} [Mg m^{-3}]	1.348	1.540	1.589	1.403	1.500
μ [mm^{-1}]	2.012	2.018	2.301	2.771	0.785
F(000)	1670	876	4476	1556	1582
cryst size [mm]	0.20 × 0.10 × 0.03	0.21 × 0.15 × 0.05	0.21 × 0.08 × 0.08	0.17 × 0.11 × 0.06	0.30 × 0.20 × 0.04
θ range [deg]	3.08−71.97	4.75−70.99	3.48−71.27	3.61−71.25	2.98−39.62
reflns collected	39193	16763	42540	34980	65698
indep reflns [R(int)]	7391 [0.0424]	3450 [0.0490]	8601 [0.0481]	6675 [0.0594]	14573 [0.0329]
obs reflns, $F_o > 4\sigma(F_o)$	6884	3130	4297	5360	13911
data/restraints/param	6884/0/530	3450/2/254	8601/24/694	6675/86/386	13911/1/458
abs struct param					−0.392(5)
extinction coeff			0.000043(18)		
GOF on F^2	1.125	1.043	1.149	1.069	1.037
final R1, wR2 [$I > 2\sigma(I)$][a,b]	0.0836, 0.2190	0.0448, 0.1250	0.0622, 0.2010	0.0575, 0.1670	0.0267, 0.0739
final R1, wR2 (all data)[a,b]	0.0873, 0.2216	0.0483, 0.1306	0.1107, 0.2466	0.0669, 0.1743	0.0287, 0.0748
max, min diff [e Å^{-3}]	1.441 and −0.756	0.699 and −0.703	0.663 and −0.996	0.336 and −0.786	0.848 and −0.480
on w:[b] a, b	0.0809, 18.3859	0.0905, 0.4784	0.1202, 0.0000	0.1162, 0.4780	0.0406, 0.4450
abs correction max/min	1.000000/0.737830	0.91862/0.70543	0.88179/0.69623	0.85808/0.69306	1.000000/0.895952

[a] $R1 = \sum||F_o| - |F_c||/\sum|F_o|$. [b] $wR2 = [\sum\{w(F_o^2 - F_c^2)^2\}/\sum\{w(F_o^2)^2\}]^{1/2}$, on $w = 1/[\sigma^2F_o^2 + (aP)^2 + bP]$, and $P = (F_o^2 + 2F_c^2)/3$.

slow diffusion of a solution of the ligand into a solution of the corresponding copper(II) salt. In all three cases, single crystals suitable for X-ray crystallographic studies were easily obtained within 3 days (Table 1).

The crystal structure of **1** demonstrated it to be a 2D coordination network with formula $\{[Cu(\mathbf{L^1})_2(H_2O)Cl][Cl]\}_n$. In **1**, the copper(II) centers have octahedral geometry, being coordinated to a water molecule, to a chloride (trans to the water), and to four pyridyl groups from four different $\mathbf{L^1}$ ligands (see Figure S1 in the Supporting Information). Each of the four coordinated $\mathbf{L^1}$ molecules forms a bridge to a neighboring copper(II) center, generating a 2D infinite assembly of metallasquares with a copper(II) center in each of the vertexes (see Figure 1). The dimensions of these metallasquares, taking the Cu···Cu distance as a measure of their edges, is ca. 15 × 15 Å, giving an area of ca. 225 Å^2. However, it is important to point out that the real potentially empty space in these cavities is much smaller than that if one takes into account the van der Waals radii of the atoms that form the squares.

The 2D layers stack in an alternating fashion and are not exactly on top of each other (see Figure 1b), a characteristic derived from the octahedral geometry adopted by the metal complex. The presence of axial ligands (water and chloride) coordinated to the copper prevents two metals from being positioned one directly above the other and, hence, an offset assembly of the layers is observed. Despite the relatively large cavities generated, the grids are not interpenetrated. Consequently, their stacking allows the generation of wide and well-defined channels where several molecules of solvent are trapped (see Figure 2a for the framework with the solvent molecules included and Figure 2b for that without the water molecules).

If the sample measured is directly extracted from water, 20 different positions of water can be localized in the structure (see Figure 2a). In spite of the fact that the positions of water have different occupation ratios and are disordered, the hydrogen position of the water molecules could be partly localized. The water molecules are interconnected through hydrogen bridges, with the shortest contacts to the framework being O2···O3W (2.7 Å), O3···O5W (2.7 Å), Cl1···O3W (3.1 Å), N2···O6W (3.0 Å), N3···O2W (3.1 Å), N6···O8W (2.9 Å), and N7···O15W (3.2 Å) (see the Supporting Information for details on the numbering scheme). Because of the large number of water molecules inside the cavities and the fact that they are disordered, it has not been possible to find the noncoordinated chloride anions (one per copper center) that should be located inside the cavity.

The reaction between $Cu(OAc)_2$ and $\mathbf{L^1}$ yields another 2D metalla-assembly with the formula $\{[Cu(\mathbf{L^1})(CH_3COO)_2]\}_n$ (**2**). In this structure, each copper center is coordinated in a square-based pyramidal fashion by three independent $\mathbf{L^1}$ molecules and two acetate ligands. The equatorial positions are coordinated by two pyridine rings and two acetate anions,

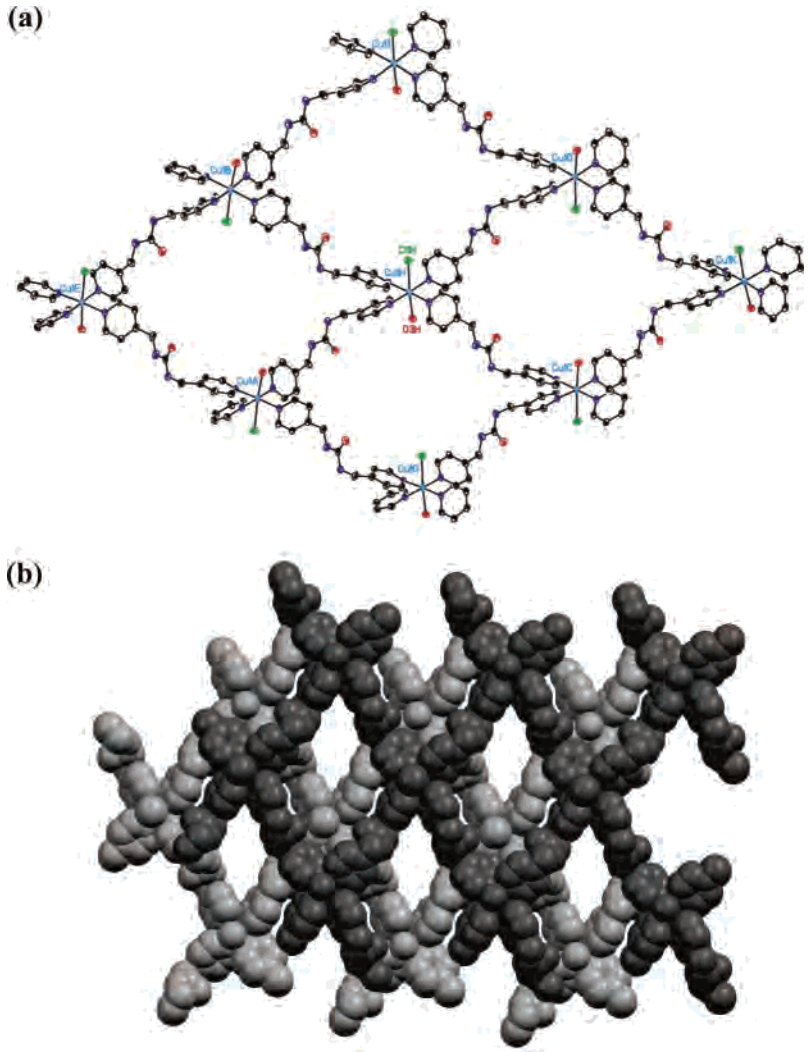

Figure 1. Coordination of $\mathbf{L^1}$ to the copper(II) centers generating (a) a 2D infinite assembly of metallasquares, which (b) stack on top of each other, generating infinite channels. Hydrogen atoms have been omitted for clarity.

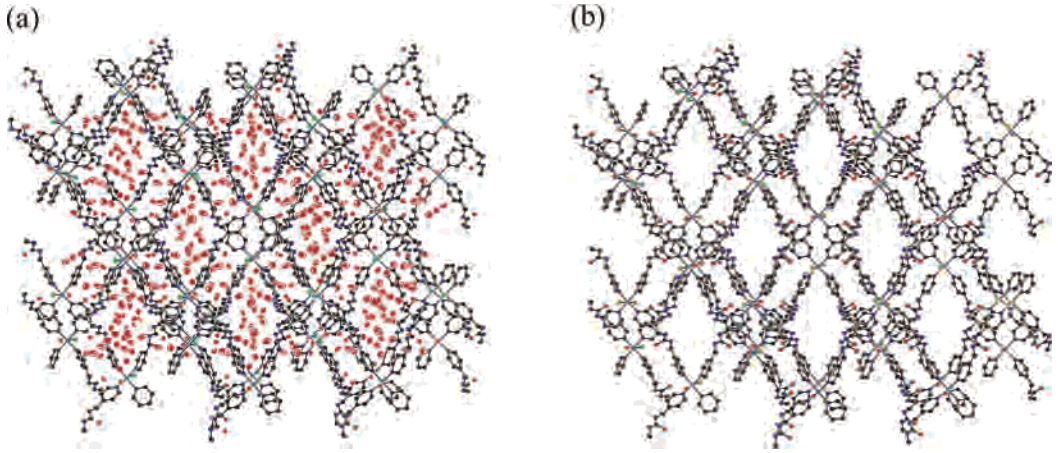

Figure 2. Representation of **1** showing the infinite channels (a) filled with water molecules and (b) with the solvents artificially removed to show the size of the empty channels. Hydrogen atoms have been omitted for clarity.

while the axial position is occupied by a third ligand coordinated via its urea's carbonyl group (see Figure 3 and Figure S2 in the Supporting Information). The coordination of each ligand $\mathbf{L^1}$ to three copper atoms via the pyridines and the oxygen of the urea group leads to the formation of a polymeric assembly of $Cu_2(\mathbf{L^1})_2$ rectangles (see Figure 3). The distance separating the two copper centers located at the vertexes of each metallamacrocycle is ca. 8.0 Å, while the distances between each copper and the carbon atoms of the two urea groups located at the two other vertexes of the rectangle are ca. 3.5 and 7.3 Å for the long and short sides, respectively.

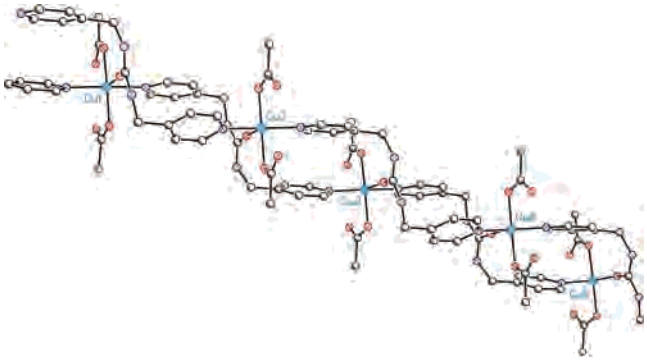

Figure 3. Partial view of the polymeric assembly of metallaboxes formed by bridging of the copper centers with **L**[1] via the pyridyl (in the equatorial positions) and urea (axial position) groups of the ligand. Hydrogen atoms have been omitted for clarity.

An interesting feature of this assembly is that the polymeric chains of rectangles interact with each other via hydrogen bonds. The urea groups act as hydrogen bond donors, establishing bridges with the oxygen atoms of the coordinated acetate groups (N8···O19, 2.8 Å; N10···O22, 2.8 Å) and generating the expanded structure shown in Figure 4.

To study further the influence of anions on the final structure of the copper−**L**[1] assemblies, it was decided to use a counterion with a tetrahedral geometry (in contrast to chloride and acetate) and with a different coordinating ability. Thus, the reaction between $CuSO_4$ and **L**[1] was carried out, yielding yet a different type of metal−organic network with formula $\{[Cu(\mathbf{L^1})_2(H_2O)_2][SO_4]\}_n$ (**3**). In this case, each copper(II) center is coordinated to four independent **L**[1] ligands via their pyridyl groups and to two water molecules, giving an octahedral geometry. Each ligand bridges two different metals, yielding layers formed by repeating boxes of $Cu_2(\mathbf{L^1})_2$ in which each copper center is shared by two neighboring boxes (see Figure 5a). In contrast to the structures of **1** and **2**, in the structure of **3**, the anion (i.e., SO_4^{2-}) is not coordinated to any of the copper(II) centers. Instead, each sulfate interacts via hydrogen bonds with two copper-coordinated H_2O molecules and with the urea groups of two different **L**[1] ligands (each of which comes from a neighboring box; distances O11···N8, 3.26 Å; O11···N10, 3.01 Å; O12···O1(water), 2.73 Å; O12···N8, 2.94 Å; see the Supporting Information for the numbering scheme). It is not unlikely that the sulfate anion somehow directs the packing of the polymeric layers of boxes, leading to the structure shown in Figure 5b.

The different nature of the assemblies described in this section clearly shows the important role played by the counteranions in defining the overall structure of metal−organic frameworks. Each anion has different coordinating abilities and, hence, can influence directly the coordinating environment of the metal center, as can be seen in assemblies **1** and **2** with chloride and acetate, respectively. On the other hand, the geometry and size of the anionic species can play an important role in determining the structure of the assembly by establishing supramolecular interactions with the components of the system, as is the case of the noncoordinated sulfate anion in **3**.

Synthesis and Single-Crystal X-ray Structures of 4 and 5. To investigate further the influence that different anions have on the final structure of the infinite metal−organic assemblies, we investigated the reactions between the same three copper salts and the slightly different ligand **L**[2] (see Scheme 2). The only difference between **L**[1] and **L**[2] is the relative position of the nitrogen in their pyridyl rings.

The reactions of **L**[2] with $CuCl_2$, $Cu(OAc)_2$, and $CuSO_4$ were carried out (and compared to the previously reported structure resulting from the reaction between $Cu(NO_3)_2$ and **L**[2]). Unfortunately, despite several crystallization attempts, it was not possible to determine the X-ray crystal structure of the assembly resulting from the reaction between **L**[2] and

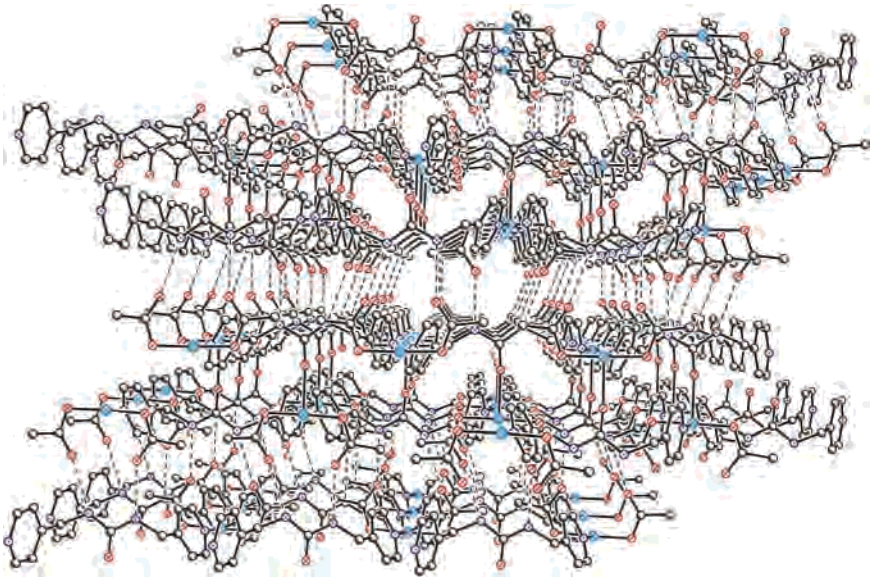

Figure 4. View of the packing in the structure of **2**. The urea groups of the coordinated **L**[1] ligands (of one layer) act as hydrogen-bond donors, establishing bridges with the oxygen atoms of the coordinated acetates (in the adjacent layer) and generating an expanded 3D structure. Hydrogen atoms have been omitted for clarity.

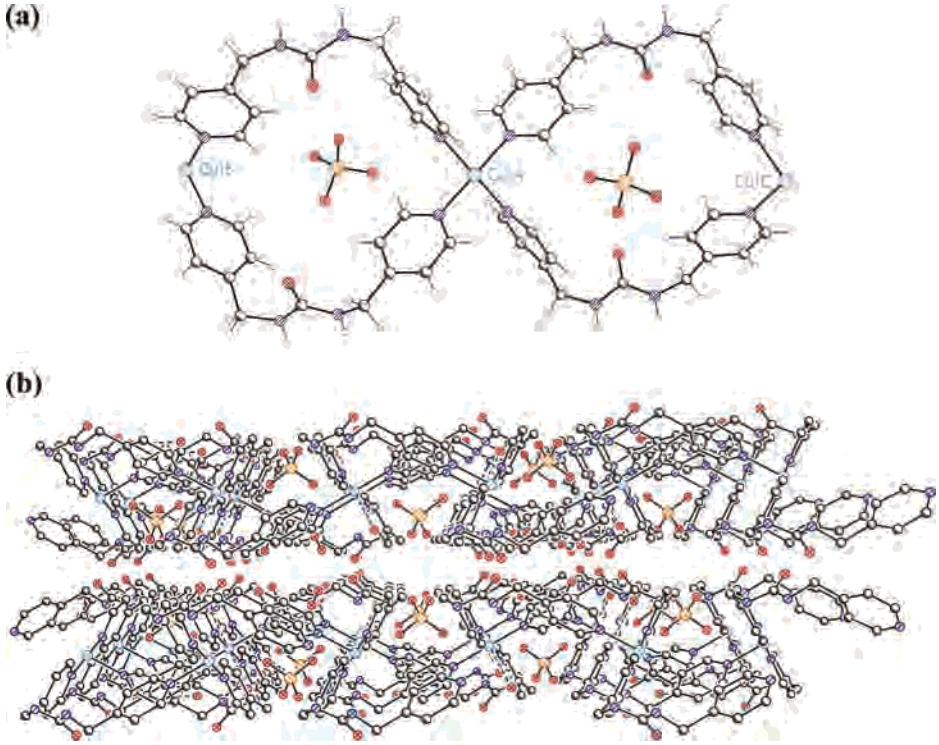

Figure 5. (a) In **3**, the copper centers coordinated to four different bridging $\mathbf{L^1}$ ligands, yielding a polymeric arrangement of metallaboxes. The sulfate anions are not coordinated but located above the metallaboxes. (b) View of the crystal packing of the structure of **3** showing the position of the sulfate anions and the stacking of the 2D layers.

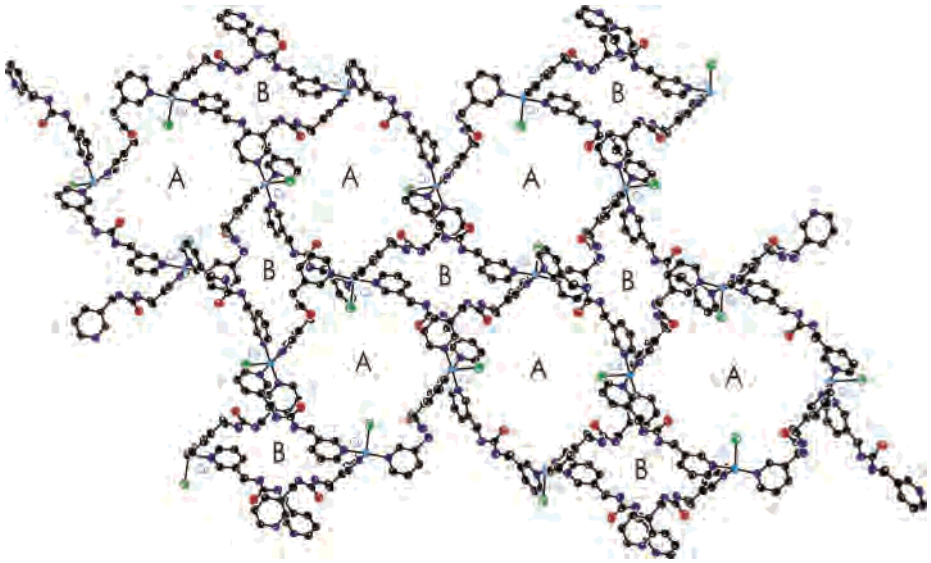

Figure 6. View of one of the 2D layers formed by coordination of $\mathbf{L^2}$ to $CuCl_2$. In this structure, two different types of boxes (A and B) are formed. Hydrogen atoms have been omitted for clarity.

$Cu(OAc)_2$, and hence only the metal assemblies obtained with the two other copper(II) salts will be discussed.

The reaction between $CuCl_2$ and $\mathbf{L^2}$ leads to the formation of an infinite assembly of metallaboxes with formula $\{[Cu(\mathbf{L^2})_2Cl_2]\}_n$ (**4**). The copper(II) center in this species has a distorted octahedral geometry, coordinating four $\mathbf{L^2}$ ligands via the pyridyl groups in the same plane and two chloride anions in the axial position. The coordination of the two chloride anions in **4** is asymmetric, with the Cu−Cl distances differing by 0.43 Å (Cu1−Cl1, 2.634 Å; Cu1−Cl2, 3.067 Å; see Figure S4 in the Supporting Information).

This coordination geometry leads to the formation of 2D infinite layers in which there are two different types of $[Cu_4L_4]$ metallaboxes, A and B (see Figure 6). These rings differ in the relative folding of the bridging ligands, although the dimensions of the boxes are practically the same: ca. 11 × 12 Å in each case (with the diagonal Cu···Cu distances for ring A being 15.2 and 16.7 Å and those for ring B being 15.8 and 16.0 Å). As in the structure of **1**, in **4** there is no interpenetration between neighboring layers, generating large cavities with the potential for inclusion of molecules. The extensive disorder in the included solvent in the structure of

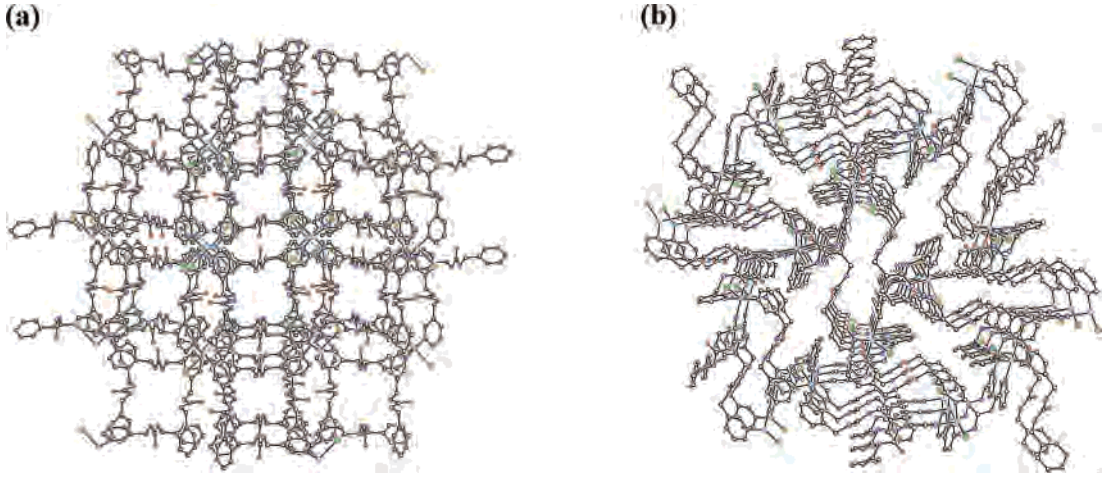

Figure 7. Two different views of the infinite channels formed in **4**. Hydrogen atoms have been omitted for clarity.

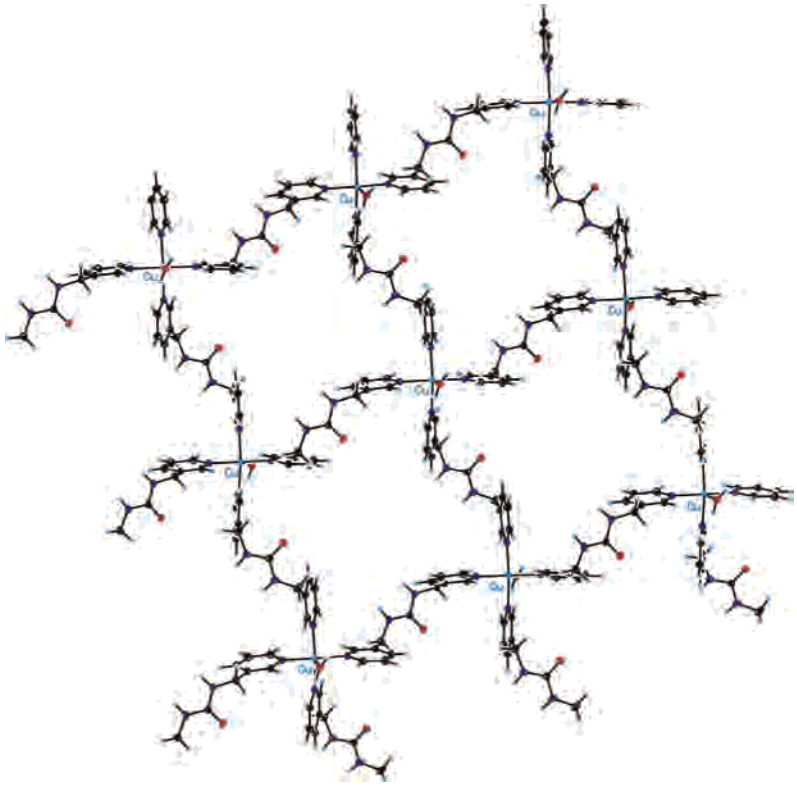

Figure 8. View of the 2D layers formed by coordination of $\mathbf{L^2}$ to $CuSO_4$.

4 led to application of a technique that deletes the solvent contribution from the X-ray data. Although the location of the solvent molecules was hence precluded (see the Experimental Section), observations before this technique was employed clearly showed solvent lying within the cavities.

The infinite 2D layers formed by the copper(II) centers and the bridging $\mathbf{L^2}$ ligands are piled on top of each other, generating infinite 3D channels in two different directions (see Figure 7a,b).

The large cavities and infinite channels observed in this structure are attractive features with the potential for the use of crystalline samples of **4** as a nanoporous material for the storage of small molecules. As discussed later, this assembly has a relatively high thermal stability and hence could lead in the future to interesting applications.

Finally, the reaction of $\mathbf{L^2}$ with $CuSO_4$ yields the assembly $\{[Cu(\mathbf{L^2})_2(H_2O)][SO_4]\}_n$ (**5**) in which the copper(II) center has a square-based pyramidal geometry. Each metal center is coordinated to the pyridyl groups of four different $\mathbf{L^2}$ ligands and to one water molecule (see Figure S5 in the Supporting Information). This coordination geometry generates infinite 2D layers of identical $[Cu_4L_4]$ metallaboxes (see Figure 8).

In contrast to the structures described so far, in this metal−organic assembly two 2D layers interpenetrate, generating a tight-knitted self-filling network (see Figure 9).

The interpenetration of the layers prevents the sulfate anions and the solvent molecules from being positioned inside the $[Cu_4L_4]$ rings, and as a consequence, they are found between the layers (see Figure 10). For each copper atom, it

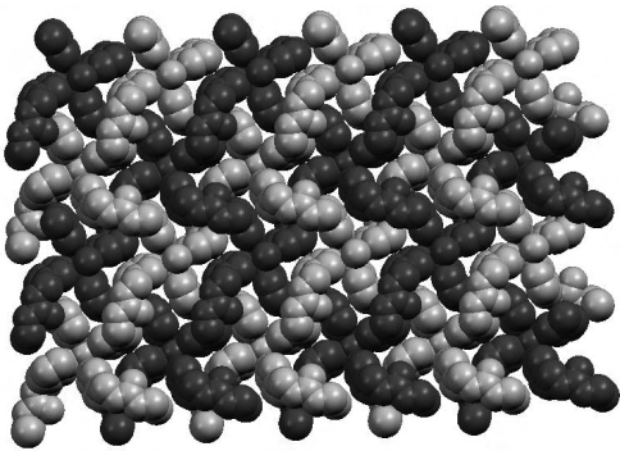

Figure 9. Space-filling representation of the interpenetration of two of the 2D layers in the structure of **5**. Hydrogen atoms have been omitted for clarity.

was possible to localize one sulfate anion and nine different water positions (with the water molecules being partly disordered with different occupation ratios). The 2D grids are connected to each other through hydrogen bonds involving the sulfate anions and the water molecules. The shortest contacts between the sulfate counterions and the urea groups of $\mathbf{L^2}$ in the grids are N5···O2 of 2.92 Å and N2···O3 of 2.93 Å (see the Supporting Information for the numbering scheme).

The structures of the metalla-assemblies **4** and **5** show again the important role played by the counteranions in defining the nature of the assemblies. While chloride coordinates to the copper centers to yield **4** (such as those of the nitrate anion in the previously reported structure $[Cu(\mathbf{L^2})_2(NO_3)_2]$), sulfate remains as a counterion in **5**. In the latter, the anion is located between the 2D layers, forming hydrogen bonds with the urea groups of $\mathbf{L^2}$. Interestingly, the slight difference in the relative position of the urea and pyridyl groups of $\mathbf{L^2}$ in comparison to $\mathbf{L^1}$ seems to be enough to change the overall arrangement of the 2D layers. While in **3** there is no interpenetration of the grids, the structure of **5** shows interpenetration of the metal−organic grids.

TGA. To study the thermal stabilities of the five copper(II) assemblies **1**−**5**, the samples were analyzed by TGA. Crystalline samples of the corresponding metal−organic network were taken out of solution and left to dry in a desiccator for 24 h, ensuring that the surface of the crystals was not wet with solvent from the mother liquor. The resulting dry samples were then analyzed by TGA. Upon heating, samples of **1**, **3**, and **5** show the first weight loss at around 100 °C (between 6.6 and 11.2% of the mass of the corresponding sample). As shown by their X-ray crystal structures, all of these samples contain a considerable amount of solvated water in their crystalline structure, and hence it was expected to see a considerable weight loss at this temperature. In the case of complex **4**, a gradual weight loss of approximately 4% occurs between 70 and 120 °C, which should correspond to the combined loss of methanol and water (which are the solvents used in the crystallization of the sample). For sample **2**, the first weight loss is observed at 200 °C, which is consistent with the fact that no solvent molecules were found in the X-ray crystal structure of this coordination polymer. In **1** and **3**−**5**, after the initial weight loss associated with the solvent molecules, minimal weight loss was observed up to around 250 °C, indicating that these samples are thermally stable up to these temperatures. These are encouraging results if these metal−organic assemblies are to be employed in the future for gas storage or catalysis (although it should be pointed out that thermal stability does not imply that the crystallinity of the samples is retained).

X-ray Powder Diffraction Studies. To investigate whether the crystallinity of the systems under study was retained upon increasing the temperature (to remove the entrapped solvent

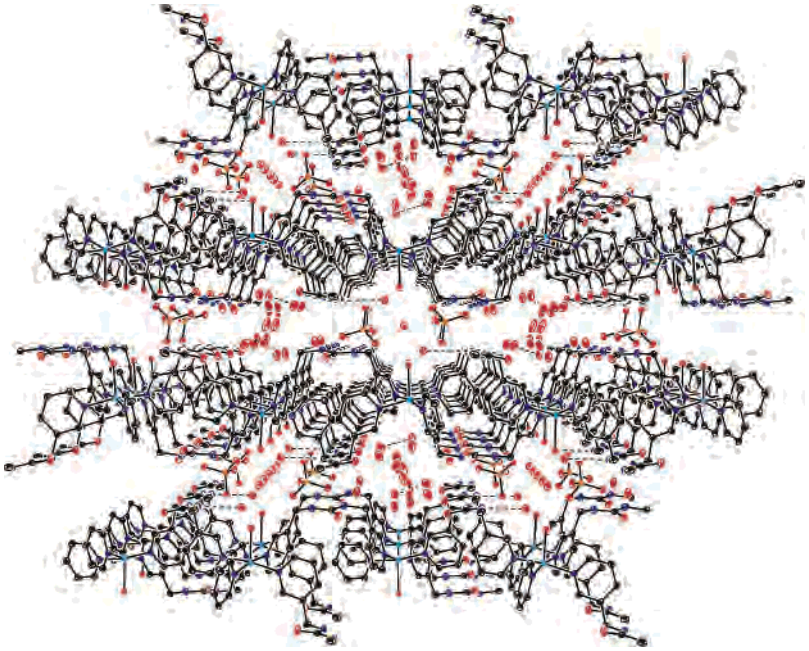

Figure 10. View of the 2D grids in **5** connected to each other through hydrogen bonds involving the sulfate anions and the coordinated water molecules. Hydrogen atoms have been omitted for clarity.

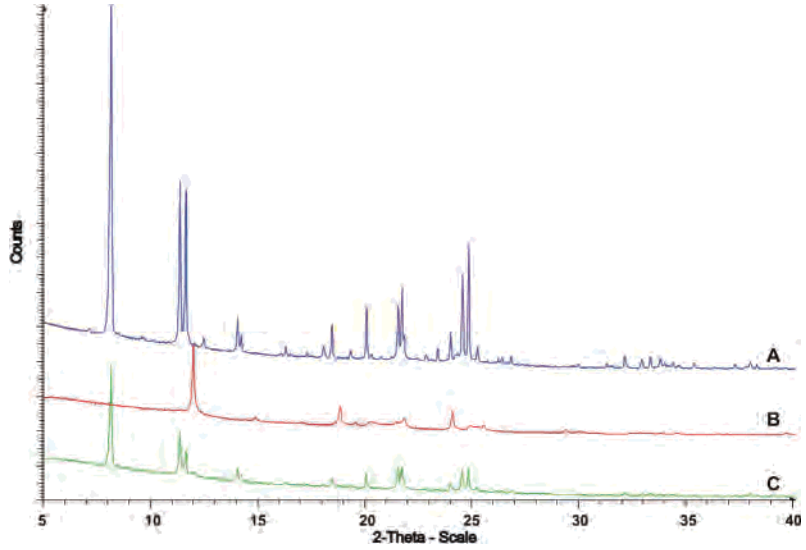

Figure 11. X-ray powder diffraction patterns of a microcrystalline sample of **4** (A), of the same sample after heating it up to 150 °C for 30 min (B), and after cooling of the sample in the presence of traces of water (C).

molecules from the framework), a microcrystalline sample of one of them (**4**) was analyzed using X-ray powder diffraction. The diffraction pattern obtained at room temperature (see Figure 11A) is consistent with the one simulated from the single-crystal X-ray diffraction study (see Table S1 in the Supporting Information for a comparison of the peaks). Once the X-ray powder diffraction pattern of **4** was established, the same microcrystalline sample was heated for 30 min up to 150 °C to remove the molecules of solvent entrapped in the metal−organic framework (see the TGA results, which show that at this temperature most of the initial mass loss due to entrapped solvents has taken place). In this process, it was noticed that the sample changed its color from dark blue to green. The X-ray powder diffraction (at room temperature and avoiding contact with moisture of the air) of this compound was carried out again. As can be seen in Figure 11, the initial diffraction pattern of **4** (plot A) changes, but the sample remains crystalline (plot B). The same sample was then treated with a few microliters of water (added with a syringe) and left to stand for 30 min at room temperature. Interestingly, the sample changed its color from green to dark blue, and the original diffraction pattern of **4** was obtained again (see plot C in Figure 11), indicating that the original structure reforms upon exposure to traces of water.

These results suggest that upon heating to 150 °C the solvent molecules entrapped in **4** are removed. As a consequence, the structure of the framework is modified but, interestingly, the crystallinity is retained. The process seems to be reversible because the presence of traces of water allows one to convert the green sample to the original compound (blue and with the diffraction pattern associated with **4**).

Conclusions

The aim of the investigations presented in this paper was to study the influence of different anions on the overall structure of various metal−organic frameworks. From the five crystal structures obtained, it is clear that the geometry and size of the anion together with its ability to interact with the metal center or with hydrogen bond donor groups, are essential in determining the structure of the metal assembly. While chloride and acetate coordinate to the copper(II) centers in **1**, **2**, and **4**, sulfate remains as a noncoordinating counterion, interacting via hydrogen bonding with the urea groups of both ligands in **3** and **5**. Regarding the geometrical differences between $\mathbf{L^1}$ and $\mathbf{L^2}$, we have shown that a small change in the relative position of the pyridyl and urea groups can lead to quite different structures. The most striking difference is between assemblies **3** and **5**. Although in both cases 2D grids are formed, in the latter the grids are interpenetrating, forming an assembly with little space to encapsulate any molecule.

From the five assemblies prepared and structurally characterized, **1** and **4** are the most promising in terms of potential applications as nanoporous materials. In these assemblies, noninterpenetrating 2D grids with relatively large cavities are formed. These cavities have been shown to be filled by solvent molecules and, in the case of **1**, by a chloride counterion. Preliminary X-ray powder diffraction studies indicate that **4** changes to a different crystalline structure upon heating at 150 °C (the temperature at which the sample is desolvated according to TGA). Interestingly, the original structure of **4** reforms upon exposure of the sample to traces of water.

Experimental Details

Materials. All of the copper(II) salts were purchased from commercial sources and used without further purification. Organic solvents with analytical purity were supplied by commercial sources and used as received. Ligands $\mathbf{L^1}$ and $\mathbf{L^2}$ were prepared according to previously reported synthetic procedures.[37,38]

Synthesis of $\{[Cu(L^1)_2(H_2O)Cl][Cl]\}_n$ **(1).** A solution of $\mathbf{L^1}$ (29.6 mg, 0.1223 mmol) in methanol (ca. 2 mL) was carefully layered on top of a 4-mL aqueous solution of $CuCl_2 \cdot 2H_2O$ (10.4

(38) Kane, J. J.; Liao, R.-F.; Lauher, J. W.; Fowler, F. W. *J. Am. Chem. Soc.* **1995**, *117*, 12003.

mg, 0.0610 mmol). Deep-blue crystals from the solution were obtained after 2 days at room temperature. One of the crystals was picked and used to determine the X-ray crystal structure. The bulk of the crystals was filtered off, washed with distilled water and methanol, and left to dry in a desiccator overnight. Yield: 21.4 mg, 50%. Anal. Calcd for $C_{26}H_{30}N_8O_3Cl_2Cu$: C, 49.01; H, 4.71; N, 17.59. Found: C, 49.02; H, 4.83; N, 17.45. IR (ν_{max}/cm^{-1}, Nujol): 3314, 3218 (−NH−, H_2O), 1674, 1646, 1614, 1548 (−NHCO).

Synthesis of {[Cu(L^1)(CH$_3$COO)$_2$]}$_n$ (2). A solution of **L^1** (18.1 mg, 0.0748 mmol) in distilled water (ca. 3 mL) was mixed with a ca. 1-mL aqueous solution of [NBu$_4$][CH$_3$COO] hydrate (40.5 mg, 0.1343 mmol). The reaction mixture was stirred for a few minutes, and Cu(CH$_3$COO)$_2$·H$_2$O (7.5 mg, 0.0376 mmol) was added to it as a solid. The mixture was left stirring for 15 min and then left to crystallize at room temperature. Blue crystals were obtained from the solution after 1 day. One of the crystals was picked and used to determine the X-ray crystal structure. The bulk of the crystals were filtered off, washed with distilled water, and left to dry in a desiccator overnight. Yield: 8 mg, 46%. Anal. Calcd for $C_{17}H_{20}N_4O_5$-Cu: C, 48.15; H, 4.80; N, 13.27. Found: C, 48.15; H, 4.80; N, 13.27. IR (ν_{max}/cm^{-1}, Nujol): 3348 (−NH−), 1664, 1587, 1557 (−NHCO−).

Synthesis of {[Cu(L^1)$_2$(H$_2$O)$_2$][SO$_4$]}$_n$ (3). A solution of **L^1** (12.2 mg, 0.0504) in distilled water (ca. 6 mL) was carefully layered on top of 5 mL of an aqueous solution of CuSO$_4$·5H$_2$O (12.6 mg, 0.0505 mmol). Violet crystals were obtained from the pale-blue solution. One of the crystals was picked and used to determine the X-ray crystal structure. The bulk of the crystals was filtered off, washed with distilled water and methanol, and left to dry in a desiccator overnight. Yield: 13.1 mg, 33%. Anal. Calcd for $C_{26}H_{32}N_8O_8SCu$: C, 45.91; H, 4.71; N, 16.48. Found: C, 45.91; H, 4.72; N, 16.42. IR (ν_{max}/cm^{-1}, Nujol): 3265 (br, −NH−, H_2O), 3135, 3107, 3048, 3027 (−CH$_2$−), 1648, 1622, 1585 (−HNCO−), 1113−1028 (br, SO_4^{2-}).

Synthesis of {[Cu(L^2)$_2$Cl$_2$]}$_n$ (4). A solution of **L^2** (27.1 mg, 0.1057 mmol) in methanol (ca. 1 mL) was carefully layered on top of 3 mL of an aqueous solution of CuCl$_2$·2H$_2$O (9.1 mg, 0.0534 mmol). Blue crystals from the solution were obtained after 2 days at room temperature. One of the crystals was picked and used to determine the X-ray crystal structure. The bulk of the crystals was filtered off, washed with distilled water and methanol, and left to dry under reduced pressure at ca. 100 °C. Yield: 17.9 mg, 59%. Anal. Calcd for $C_{26}H_{28}N_8O_2CuCl_2$: C, 50.44; H, 4.53; N, 18.11. Found: C, 50.33; H, 4.54; N, 18.00. IR (ν_{max}/cm^{-1}, Nujol): 3320 (−NH−, H_2O, br), 1643 (br), 1608, 1568 (br, −NHCO−).

Synthesis of {[Cu(L^2)$_2$(H$_2$O)][SO$_4$]}$_n$ (5). Ligand **L^2** (20.3 mg, 0.0792 mmol) was dissolved in ca. 3 mL of hot distilled water. To this solution was added CuSO$_4$·5H$_2$O (19.8 mg, 0.0793 mmol) as a solid, and the mixture was stirred for ca. 15 min and then left at room temperature to crystallize. Blue crystals were obtained from the solution in 1 day at room temperature. One of the crystals was picked and used to determine the X-ray crystal structure. The bulk of the crystals was filtered off, washed with distilled water and methanol, and left to dry in a desiccator overnight. Yield: 22 mg, 75%. Anal. Calcd for $C_{26}H_{28}N_8O_6SCu$: C, 45.91; H, 4.71; N, 16.48. Found: C, 45.89; H, 4.25; N, 16.42. IR (ν_{max}/cm^{-1}, Nujol): 3304, 3264 (br, −NH−, H_2O), 1654 (−HNCO−), 1109, 1058, 1044 (SO_4^{2-}).

Crystal Structure Determinations. Measurement of **1** was carried out on a Bruker-Nonius diffractometer equipped with a Proteum CCD area detector, a FR591 rotating anode with Cu Kα radiation, Montel mirrors as the monochromator, and a Kryoflex low-temperature device (T = 90 K). Software: data collection, Proteum version 1.37 (Bruker-Nonius 2002); data reduction, Saint Plus version 6.22 (Bruker-Nonius 2002); absorption correction, SADABS version 2.03 (2002), structure solution and refinement, SHELXTL version 6.12 (Sheldrick 2000). Measurements of **2**−**4** were performed on an Oxford Diffraction Xcalibur PX Ultra diffractometer using Cu Kα radiation and an Oxford Instruments Cryojet low-temperature device (T = 173 K). The structures were solved and refined using the SHELX-97 program system. The included solvent in the structure of **4** was disordered over numerous partial occupancy sites, and so the SQUEEZE procedure was used.[39] The solvent was assigned as water because the original electron peaks seemed to resemble this solvent more than methanol (the other solvent used). Measurement of **5** was performed using a Bruker-Nonius diffractometer equipped with an APPEX 2 4K CCD area detector, a FR591 rotating anode with Mo Kα radiation, Montel mirrors as the monochromator, and a Kryoflex low-temperature device (T = 100 K). Software: data collection, Apex2 version 1.0−22 (Bruker-Nonius 2004); data reduction, Saint+ version 6.22 (Bruker-Nonius 2001); absorption correction, SADABS version 2.10 (2003); structure solution and refinement, SHELXTL version 6.10 (Sheldrick, Universtität Göttingen, Germany, 2000).

The powder diffraction patterns of **4** were measured in transmission using a D8 Bruker-Nonius device equipped with a copper X-ray source (1.540 64 Å).

TGA. The thermal decomposition of the products was studied by means of TGA on a Mettler Toledo TGA/SDTA851 instrument in a temperature range between 30 and 600 °C. For all thermal analyses, the heating rate was 10 °C/min.

Acknowledgment. We thank EPSRC (U.K.) and the ICIQ Foundation for financial support. P.D. thanks EPSRC (U.K.) and the Ministerio de Ciencia y Tecnologia (Spain) for postdoctoral fellowships. Susana Delgado and Eduardo C. Escudero are thanked for their help with the TGA and X-ray powder diffraction measurements, respectively.

Supporting Information Available: TGA data of **1**−**5**, X-ray crystallographic structures for **1**−**5**, X-ray powder diffraction for **5**, and a CIF file containing the crystallographic information. This material is available free of charge via the Internet at http://pubs.acs.org.

IC051457I

(39) Sluis, P. v. d.; Spek, A. L. *Acta Crystallogr., Sect. C* **1990**, *A46*, 194.